Original Paper   **Open Access**

Maize cell wall degradability, from whole plant to tissue level: different scales of complexity

Mary S-J Wong Quai Lam[1], Yves Martinez[2], Odile Barbier[1], Alain Jauneau[2], Magalie Pichon[1]*

[1]CNRS - Université Paul Sabatier, UMR 5546, LRSV, 24 Chemin de Borde Rouge, 31326 Castanet Tolosan, France
[2]Plateforme de microscopie - FR AIB (Agrobiosciences, Interactions, Biodiversity) FR 3450 CNRS, 24 chemin de Borde Rouge, 31326 Castanet Tolosan, France
*Corresponding author: E-mail: magalie.pichon@toulouse.inra.fr
*current address: INRA, Laboratoire des Interactions Plantes Micro-organismes (LIPM), 24, chemin de Borde Rouge, Auzeville, CS52627, 31326 Castanet Tolosan, France

Abstract

Today, maize stover can be considered as a model for investigating secondary cell wall formation in grasses with major applications in cattle feeding (forage maize) and green energy production (bioethanol, biogas, etc). Up until now, cell wall formation and cell wall degradability have been considered at the whole plant scale. However, a detailed examination of leaves and internodes has underlined a large diversity of lignified cell types (xylem vessels, parenchyma, sub-epidermal and perivascular sclerenchyma) and significant variations in the organization and / or the composition of these different cell types. In this review, we highlighted several aspects of this complexity and their consequences on valorization processes both in agriculture or industries.

Keywords: *Zea mays*, cell wall digestibility, anatomy, sclerenchyma, parenchyma

Introduction

Recent economical and environmental contexts have greatly strengthened the necessity of producing in sustainable ways substitutes to fossil fuels. An important "tank" for biofuel in future is yet based on the use of lignocellulose products. Maize (*Zea mays* L) is one of the most widely grown crops in the world to produce grain and silage. In maize dedicated to grain production, the use of mature stalks as resources for second generation biofuels appears to be a good compromise allowing energy production without competition with food availability. Moreover, due to its great facilities for plant selfing and crossing, its large genetic resources, and the considerable genetic backgrounds and genomic tools, maize is the most efficient model plant for the improvement of all C4 grasses (sorghum, switchgrass, sugarcane, miscanthus, etc) considered for industrial biomass production.

Although plant biomass is often considered as having a uniform composition, there is in fact a substantial diversity linked to different factors. First, different species of plants have significant differences in the proportions of cellulose, hemicelluloses, and lignins found in their biomass and secondly, the types of hemicelluloses and/or the ratios of monomers in lignins vary greatly (Burton et al, 2012). In addition to these species-specific differences, the average composition of a single species can vary regarding the organ considered. For example, in maize root, the monomeric composition of lignins are particularly S unit rich whereas leaves contain high proportion G

unit (Guillaumie et al, 2007). At a lower scale, every plant consists of many different cell types, each with a unique cell wall that contains qualitative and local structural differences in their components (Kieran et al, 2011). For all these reasons, we need to consider this compositional complexity of plant feedstock when evaluating and assessing the robustness of technical processes designed for a given application.

Most knowledge of cell wall polymers is derived from the physicochemical analysis of fractionated walls and isolated polymers with the correlative loss of most spatial and developmental information. However, tools at cellular scale are now available to determine chemical signature or physical properties of cell wall cells. Indeed, wall constituents such as pectins, proteins, aromatic phenolics, cellulose, and hemicelluloses have characteristic spectral features that can be used to identify and/or fingerprint these polymers without, in most cases, the need for any physical separation. Fourier-transform infrared (FT-IR) microspectroscopy, is widely used to provide an overview of all the major chemical components in a cell wall (McCann et al, 1992; Séné et al, 1994; McCann et al, 2007). Raman spectroscopies, that have greater capacity for the spatial resolution of chemical signatures than FT-IR, are also used in cell wall studies, and have the potential to indicate differences in the orientation of cellulose microfibrils (McCann et al, 1992). Synchrotron radiation microspectroscopy (SR-IMS) and Atomic Force Microscopy (AFM) provided cellulose topography of maize cell walls (Dokken et al, 2007; Ding and Himmel, 2006). Immuno-histolog-

ical technique is currently one of the best methods to precisely locate polymers within complex tissues using different antibodies (Knox, 2008). Since a decade now, Laser Capture Microdissection (LCM) has become an ideal tool to isolate specific tissue in an organ (Kerk et al, 2003).

Regarding the nutritive value of forage crops, the botanical characteristics of the plant material are recognized as a factor determining the cell wall degradability as well as the maturation stage of plants (Walters, 1971). In the same time, it was considered that the pattern of lignin distribution, rather than the total amount of lignins, accounted for much of the variation in digestibility between forage types (McManus and Bigham, 1973). Further work confirmed the importance of anatomical features in attempting to predict the nutritive value of forages (Wilkins, 1972; Akin and Burdick, 1975). In maize, several investigations (Boon et al, 2005, 2008; Méchin et al, 2005) devoted to internode quality reported that the differences in the percentage of lignified area in the internodes between the plants was associated with differences in their in vitro dry matter degradability. Akin and Burdick (1975) have examined cool- and warm-season grasses and demonstrated differences in cell-wall structure (especially extent of lignification) between specific tissue cells and their response to rumen digestion. Schertz and Rosenow (1977) reported distinct anatomical variations between sorghum [*Sorghum bicolor* (L.) Moench] cultivars, considering number and thickness of lignified epidermis, sclerenchyma, and vascular bundle cells. Thus, combining cytological observations with digestibility properties could allow designing an anatomical ideotype well adapted to both silage use or biofuel production.

Materials and Methods

Histological stains

Sections of 130 µm thick of fixed material (ethanol 70%) were made with a vibratome (LEICA VT 1000S) on internode sections of maize plants at flowering stage. Bright field and fluorescence images were realized using an inverted microscope (Leica DM IRBE, LEICA, Germany) equipped with aTri-CCD Colour Camera (Color Cool View, Photonic Science, Milham, Germany). From embedded material (LRWhite Resin), thin sections of 1µm were performed with an ultramicrotome equipped with a diamond knife (UltraCutE, Leica, Germany). Several colorations were considered :

- Phloroglucinol-hydrochloric solution (VWR/26337.180) reveals lignins which were stained in reddish color in bright field microscopy.
- Mirande's reactif (Jeulin/fr, 10514584) allows the visualization under fluorescence of the lignin in blue and pectocellulosic components in red-pink color.
- Lugol solution (mix of I_2 and KI at 1% of iodure) was used to detect starch (blue dark color)
- Toluidine blue 0.5% in an aqueous solution 2.5% of

sodium carbonate, pH 11, is a polychromatic dye of plant cell wall components.

Immunolocalization

Experiments, including samples fixation, embedding and labeling, were performed according the article of Philippe et al (2006). Briefly, ferulate components were detected using a primary antibody (anti-5-*O*-Fer-Ara) diluted at 1/2,000 and revealed by a suitable secondary antibody Alexa 633 labelled. Visualization of the labeling was done with a spectral confocal microscope (Laser Scanning Confocal Microscope SP2, Leica, Germany).

Enzymatic degradation assay

Enzymatic hydrolysis was carried out using the cellulase from *Trichoderma reesei* [ATCC 26921, Sigma-Aldrich, C2730, activity of 1.5l Celluclast 700 EGU/g (endo-glucanase units per gram)] at a dilution of 1/100. The enzyme was prepared in 500 mM sodium acetate buffer at pH 5.0. The hydrolysis was performed on 100 µm thick cross-sections from the internode under ear harvested at flowering stage. The cross-sections were placed in wells containing 1 ml of the enzymatic solution and were placed in an incubator at 37°C. At designated time points 4 h, 24 h, 48 h and 72 h, samples were removed from the incubator for observation.

Laser Capture Microdissection

70 µm thick sections were laid down on a slide and cover by a PEN framed membrane. Microdissection of epidermal/sub epidermal sclerenchyma, vascular bundles including perivascular sclerenchyma and parenchyma was made, and isolated on different caps by using an Arcturus XT microdissector with UV and IR laser beam.

Scanning electron microcopy

Samples were fixed in 2.5% of glutaraldehyde in 50 mM sodium cacodylate buffer (24 h at 4°C). They were then dehydrated in a series of aqueous solutions of increasing ethanol concentrations. They were then critical-point dried with CO_2 as a transitional fluid, sputter-coated with gold palladium (JEO, JFC 1100) 50 nm, and then observed with an Hitachi (C450 SEM) which permit to have a resolution max of 6 nm and a magnification from 20 to 200,000 with an accelerated voltage of 20 KV.

FTIR

Sections of 14 µm thick were realized from paraffin-embedded internode at flowering stage. Infrared spectra were collected in the transmission mode, between 800 and 1,800 cm^{-1} at 8 cm^{-1} intervals, using a Magna-IR 550 spectrometer (Nicolet, Trappes, France) equipped with an IR-plan Advantage microscope (Spectra-Tech, Shelton, CT, 15 Reflachromat lens). The spectrometer was fitted with a high-sensitivity MCT detector. Ten spectra for each cell type were registered. Data treatment was realized according to Philippe et al (2006).
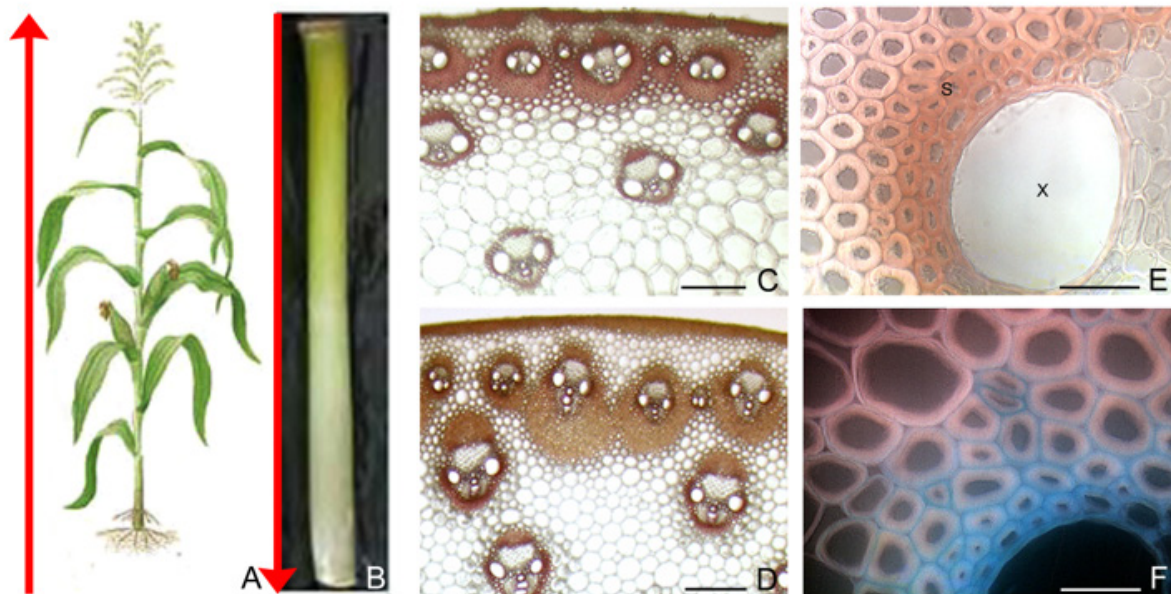
Figure 1 - Maize internode elongation and differentiation (scale bars C, D 200 μm; E, F 25 μm; s = sclerenchyma, x = xylem). A) acropetal development of plant: the oldest and the youngest internodes are at the bottom and the top of the stalk, respectively. B) an internode have a basipetal development, the younger portion is at the bottom of the internode while the older portion is at the top. C and D) Transverse sections at the top (C) and at the bottom (D) of the ear-bearing internode (phloroglucinol-HCl staining, the reddish-brown coloration indicates lignins). E) Magnification of a vascular bundle, showing the gradient of lignification from the inner to the outer parts of a perivascular sclerenchyma. F) visualization in fluorescence of cell wall compartments on section treated with Mirande's reagent (lignified walls in blue and cellulose in red-pink).

Results and Discussion

Internode development: a succession of spatial and temporal events

At the whole plant level, stems of Gramineae elongate in an acropetal mode, with two or more internodes usually elongating simultaneously or in slightly staggered succession (Morrison et al, 1994). So, the internode located at the base of the stem completes its development first (the 'oldest' internode), followed by younger internodes higher up. As a consequence there is a gradient of physiological cell wall age from the base to the top of the stem (Figure 1A).

When considering one internode, it passes through different successive development stages including cell division, cell elongation and cell differentiation. During cell division, new cells are produced by the meristem at the base of the internode. This intercalary meristematic zone remains active until the final stage of internode elongation is reached (Morrison et al, 1998). Each internode, therefore, provides a spatial resolution of the temporal events associated with secondary wall formation (Figure 1B, C, D). In the basal portion of the internode, xylem and one or two layers of sclerenchyma around vascular bundles (VB) located in the pith are heavily stained with phloroglucinol reagent (Figure 1D). In the older portion of the internode, many different cell types including epidermis, sub epidermal and perivascular sclerenchyma, and parenchyma between VB, are lignifying (Figure

1C). A closer examination of sclerenchyma surrounding VB allows observing a transversal gradient of lignification (Figure 1E). Sclerenchyma cells near the xylem are heavily stained whereas the far ones are yet pink. At cell wall level, lignification is thought to begin when secondary cell wall material starts being deposited; it serves to stiffen the cell wall, thereby fixing cell size once the cell itself is fully elongated. Deposition of lignins starts in the primary cell wall, and is then slowly extended in the direction of the cell lumen, following cellulose deposition (Figure 1F).

Internode tissue organization: a patchwork of different tissues and cell types.

Monocot stems do not have a vascular cambium, thus, they did not exhibited secondary growth. The vascular system of monocotyledons usually consists of bundles that are scattered throughout the ground tissues of the stem (Figure 2A). Different types of vascular bundles (structure and morphology) were observed in a same section. Numerous vascular bundles surrounded by sclerenchyma, were located in the ring (Figure 2B) whereas larger vascular bundles were observed in the pith (Figure 2C). Moreover, a shift in the position of the sclerenchyma surrounding the vascular bundles was observed from the top to the base of the internodes (Figure 1C, D, respectively). At the top of the stem, the sclerenchyma was roughly equally positioned on the abaxial and adaxial sides of the vascular bundles (Figure 1C). More towards the base
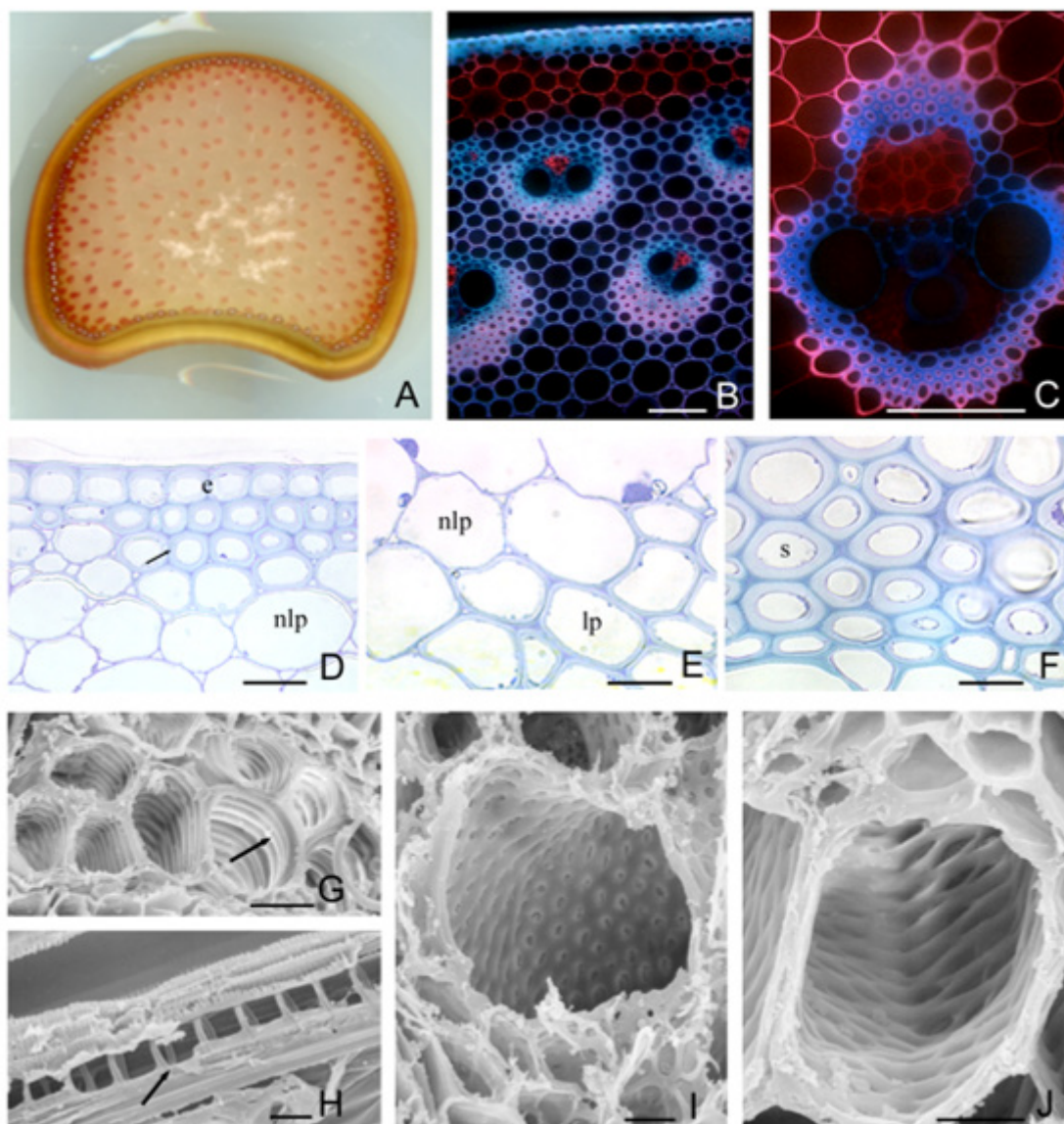
Figure 2 - Different scales of diversity in cell wall composition and structure (scale bars B 100 μm; C, D, E, F 50 μm; G, H 25 μm, I,J 10 μm; lp = lignified parenchyma; nlp = non lignified parenchyma: e = epidermis).
A) section of an ear-bearing internode phloroglucinol stained for lignin, the reddish-brown coloration indicates the presence of lignin. B and C) sections stained with Mirande's reagent. Red-pink and blue fluorescence indicate cellulosic or lignified tissues respectively. D, E, F) Images focusing on internodes cell types stained with toluidine blue. G, H, I, and J) scanning electron micrographs (transversal and longitudinal view) illustrating different lignified vessel types: G spiral and H, annealed protoxylem in vascular bundles in maize internode; I and J punctuated and reticulated vessels in metaxylem.

of the stem, sclerenchyma was predominant on the adaxial side of the vascular bundles (Figure 1D).

At the end of internode elongation, all cell types had become lignified. In epidermis, Casparian strip is deposited on radial and transverse section of the wall (Figure 2D). Immediately adjacent to epidermis, two or three layers of sclerenchyma developed thick secondary cell wall. Similarly, sclerenchyma surrounding some rind-region vascular bundles had thickened and lignified walls (Figure 2F). When considering parenchyma, different cell wall compositions were ob-

served. In the rind region between VB, small-diameter parenchyma cells developed lignified thin cell wall as post elongation development proceeded. On contrary, the parenchyma below the subepidermal sclerenchyma never lignified (Figure 2B).

At a higher scale of observation, an electron micrography of sieve-conducting xylem (mineral nutrient) allowed to visualize different types of cell wall ornamentation. In protoxylem, secondary cell wall deposition occurred by forming different ring leading to annular and spiral morphology (see arrow in
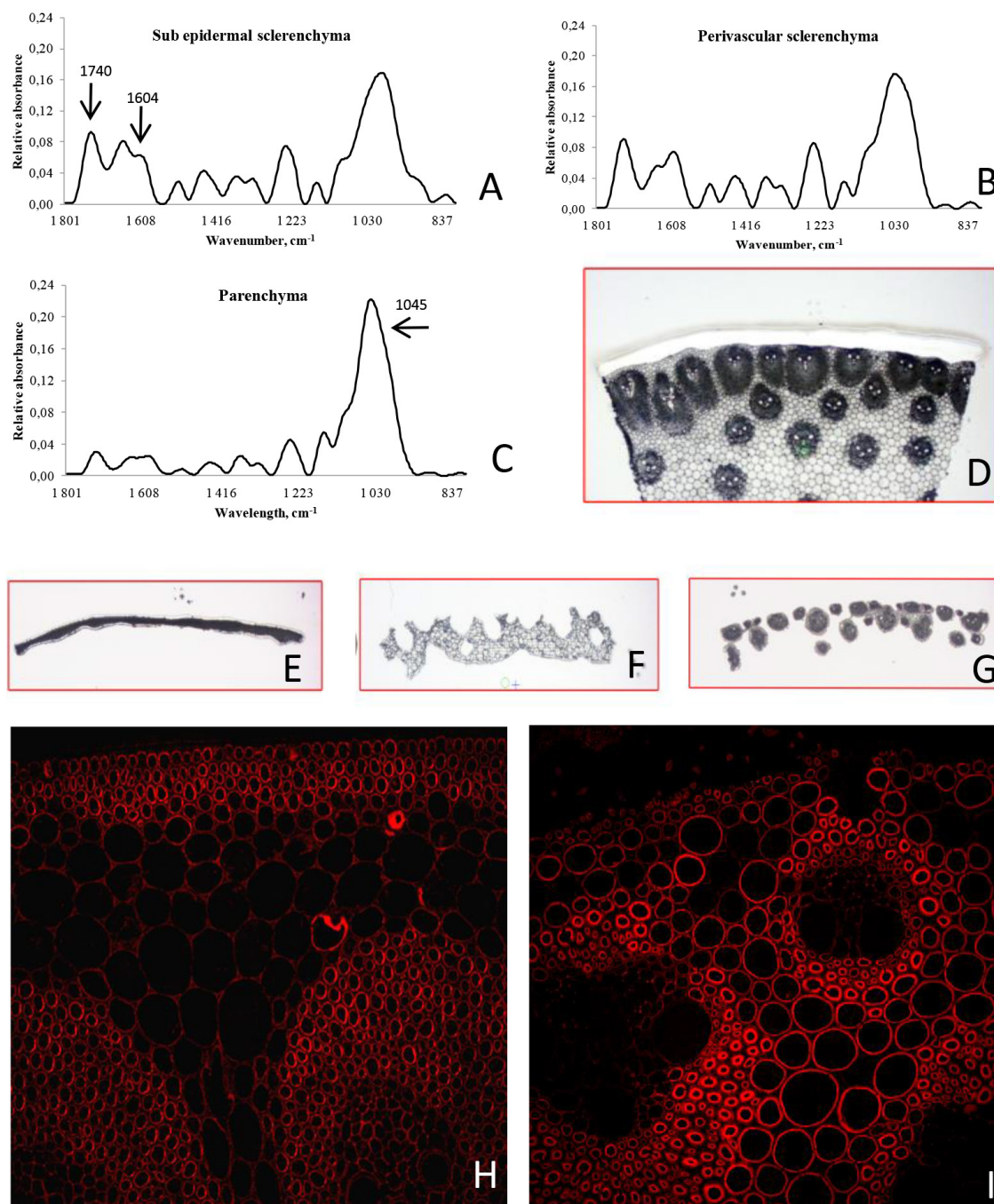
Figure 3 - *In situ* cell wall analysis (scale bars H, I 50 μm).
A-C) FTIR mean spectra of sub epidermal sclerenchyma (A), perivascular sclerenchyma (B), and parenchyma (C). In the IR region 1,200 to 900 cm⁻¹, pectins have a profile similar to that of polygalacturonic acids, and can easily be distinguished from non-pectic polysaccharides. The most diagnostic peak in the IR spectra of cell wall material is the peak centred at about 1,745 cm⁻¹, arising from the ester carbonyl stretching associated with pectin. The 1,605 to 1,635 cm⁻¹ doublet peak can be used to confirm the presence of phenolic material (Séné et al, 1994). Carbohydrates have been reported to absorb between 1,200 and 900 cm⁻¹. Atalla and Agarwal (1985) have reported that the peak at about 1,630 cm⁻¹ in the spectra of ferulic acid appears to be associated with the α–β double bond on the propanoid side group in lignin-like structures. D-G) from a whole section (D), collection by laser capture microdissection of the epidermis and sub epidermal sclerenchyma (E), vascular bundles surrounded by sclerenchyma (F), and parenchyma (G). H, I) Localization of ferulate by indirect immunofluorescence in the lower (H) and upper (I) parts of maize ear internode.

Figures 2G, H). In metaxylem, both reticulated and perforated xylem was observed (Figure 2I, J).

A variety of specific cell type composition

Different technologies have been used for studies of cell wall chemistry at cellular level. FTIR spectroscopy allows detecting the relative amounts of functional groups, including carboxyl esters, phenolic esters, amides and carboxylic acids (Séné et al, 1994). A carbohydrate fingerprint region, with absorbances at specific wave numbers, serves as diagnostic of cellulose, cross-linking glycans, and pectins in maize and other grasses (McCann et al, 1992). Fourier transform infrared (FTIR) microspectroscopy was used to get a fingerprint of wall phenotypes of different cell types in maize internodes (sub epidermal and perivascular sclerenchyma, and parenchyma) (Figure 3A-C). The surface of all peaks between 1740 cm^{-1} and 1,604 cm^{-1}, which cover the lignin absorbance, were significantly higher in sclerenchyma cell walls under epidermis and surrounding vascular bundles than in parenchyma (Figure 3A-C). On contrary, parenchyma is enriched in carbohydrates, mainly in xylans (wave number 1,045 cm^{-1}) (Figure 3C).

To go further in identifying cell wall components, cell types were separated and harvested by laser capture microdissection (LCM). LCM has been applied with success to separate lignified cells in maize coleoptile (Nakazono et al, 2003), in alfalfa (Nakashima et al, 2008), and in Arabidopsis (Ruel et al, 2009). In maize, tissues were dissected in the following steps: epidermis, vascular bundles and parenchyma (Figure 3D-G). Significant differences in lignin composition between different tissues were observed. In agreement with phloroglucinol staining (more red coloration within tissue rich in G unit), epidermis of both lines is particularly rich in G units (about 80%). Sclerenchyma around vascular bundles exhibited a S/G ratio varying between 0.56 and 0.75, according the maize line (Wong et al, in progress). As observed by Joseleau and Ruel (1997), H units were undetectable in parenchyma cells walls, and the S/G ratio was around 1.

Immuno-histochemical technique is also an interesting tool for the studies of cell wall microstructures and to locate polymers precisely in situ (Knox, 2008). Distribution of lignins in primary and secondary cell walls has been performed using immunological probes in maize coleoptiles (Müsel et al, 1997) and in internodes (Joseleau and Ruel, 1997; Tamasloukht et al, 2011). In relation with digestibility, the dynamic of ferulic acid deposition in the cell wall of maize internode was studied using a polyclonal antibody raised against ferulic acid ester linked to arabinoxylans (pAb anti-5-*O*-Fer-Ara) (Philippe et al, 2006). Indeed, grass cell walls are atypical because their xylans are acylated with ferulate and lignins are acylated with p-coumarate. Ferulic acid derived from phenylpropanoid metabolism, is found in both primary and secondary grass cell walls (Harris and Hartley, 1976). The forma-
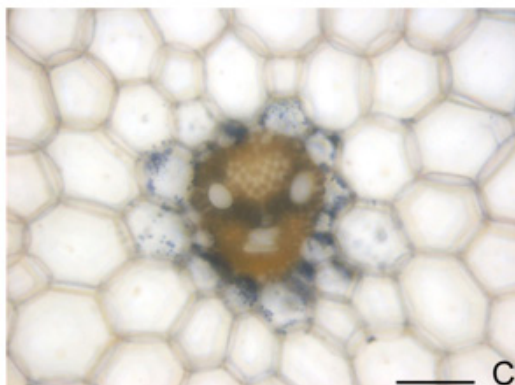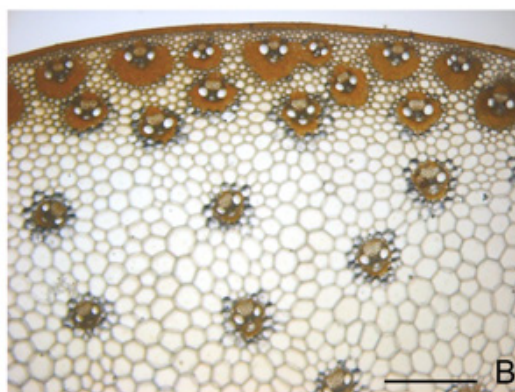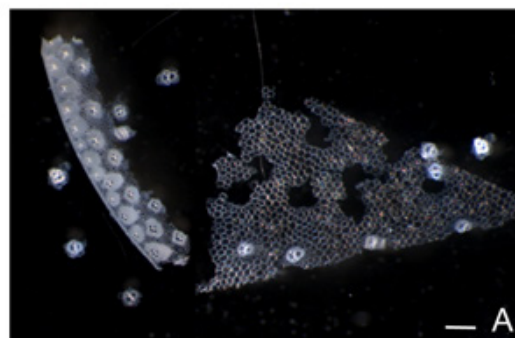

Figure 4 - Enzymatic degradation test (scale bars A,B 500 μm; C 100 μm).
A) enzymatic treated stalk section with Celluclast enzymatic reagent. B, C) lugol staining of starch (bluish-black color). Degradation is facilitated in enriched starch layers surrounding the vascular bundles.

tion of ferulate dimers occurred in vegetative organs, contributing to network formation in the cell walls of vegetative organs and thus having a potential influence on forage digestibility (Dobberstein and Bunzel, 2010). Immunolabelling of transverse sections coming from the lower and upper parts of the ear internode with a 5-*O*-Fer-Ara epitope (Philippe et al, 2006) showed a spatio-temporal deposition of ferulate (Figure 3H, I). In the lower unlignified part of the internode,

the labeling was mainly detected in the epidermis, the subepidermal and perivascular sclerenchyma (Figure 3H). As we move along the internode towards ligni- fied tissues, in the middle part, a faint labeling of the parenchyma cells between the vascular bundles was observed (data not shown). Labeling intensity was the most abundant in the upper part of the internode especially the perivascular sclerenchyma and paren- chyma cell wall (Figure 3I). Labeling was never ob- served in the xylem.

Bundle sheat layers are the first target of degrada- tion enzymes

Internode degradability has already been evalu- ated in maize in different manner, in tissues sections (Jung and Casler, 2006), or fragmentized sections (Morrison et al, 1996). Thus, Jung and Casler (2006) observed stem section of an internode at maturity af- ter in vitro degradation by rumen microbes for 24 or 96 h. They observed that pith parenchyma immedi- ately interior to the rind region of the stem was almost completely degraded within 24 h whereas the paren- chyma located in the more central pith region was less degraded, but parenchyma surrounding vascular bundles were also completely degraded. To go fur- ther in understanding the degradability of cell wall components in maize internode during stalk develop- ment, Morrison et al (1996) evaluated by liquid chro- matography the neutral sugar residues before and after fermentation of separated pith and outer rind. Degradability of wall polysaccharides declined mark- edly from the youngest internode and then leveled off or declined more slowly through the remaining internodes, especially in the pith tissue. During both fermentation times, pith of the younger internodes degraded more quickly and extensively than rind.

In attempt to define mechanisms that dictate di- gestibility at cellular level, we performed a section digestion assay (Figure 4A). These assays were an adapted version of classic in vitro digest assay (Au- frère and Michalet-Doreau, 1983). For that, we exam- ine the action of enzymes (Celluclast) on internode sections after 24 h of incubation. After 24 h, the pith parenchyma tissue was separated from the periph- eral ring region of the internode and some vascular bundles located in the pith parenchyma were de- tached (Figure 4A). The cell layer around VB which were firstly degraded corresponds to bundle sheath layer, as shown by lugol staining. Starch was subse- quently released in the medium (Figure 4B-C).

Conclusions

Cell wall degradability is a complex trait which has been largely explored in the past at whole plant level, and many data concerning biochemistry are described in the literature. This review pointed the di- versity of maize cell walls, which should be taken in consideration for agro-industrial applications. In that way, for breeding genotypes fitting better for biofuel production, new areas of investigations need to be developed in order to discover the molecular pro-

grams associated with each lignified cell type and to research regulatory genes which control the pattern- ing of lignifying tissue.

References

Akin DE, Burdick D, 1975. Percentage of tissue types in tropical and temperate grass leaf blades and degradation of tissues by rumen microorganisms. Crop Sci 15: 661-668

Atalla RH, Agarwal UP, 1985. Raman microprobe evi- dence for lignin orientation in the cell walls of na- tive woody tissue. Science 227: 636-638

Aufrère J, Michalet-Doreau B, 1983. *In vivo* digestibil- ity and prediction of digestibility of some by-prod- uctspp, 25-33. In: EEC seminar, Melle Gontrode. 26-29 September

Boon EJMC, Engels FM, Struik V, Cone JW, 2005. Stem characteristics of two forage maize (*Zea mays* L) cultivars varying in whole plant digestibil- ity II Relation between in vitro rumen fermentation characteristics and anatomical and chemical fea- tures within a single internode. NJAS - Wagenin- gen J Life Sci 53: 87-109

Boon JJ, Struik PC, Tamminga V, Engels V, Cone JW, 2008. Stem characteristics of two forage maize (*Zea mays* L) cultivars varying in whole plant di- gestibility III Intra-stem variability in anatomy, chemical composition and in vitro rumen fermen- tation. NJAS - Wageningen J Life Sci 56: 101-122

Burton RA, Fincher GB, 2012. Current challenges in cell wall biology in the cereals and grasses. Front Plant Sci 3: 130, doi: 10.3389/fpls.2012.00130

Ding S-Y, Himmel ME, 2006 The maize primary cell wall microfibril: A new model derived from direct visualization. J Agric Food Chem 54: 597-606

Dobberstein D, Bunzel M, 2010. Identification of fer- ulate oligomers from corn stover. J Sci Food Agric 90: 1802-1810

Dokken KM, Davis LC, 2007. Infrared imaging of sunflower and maize root anatomy. J Agric Food Chem 55: 10517-10530

Guillaumie S, San-Clemente H, Deswarte C, Martinez Y, Lapierre C, Murigneux A, Barrière Y, Pichon M, Goffner V, 2007. MAIZEWALL Database and de- velopmental gene expression profiling of cell wall biosynthesis and assembly in maize. Plant Physiol 143: 339-363

Harris PJ, Hartley RD, 1976. Detection of bound fe- rulic acid in cell-walls of *Gramineae* by Ultraviolet Fluorescence Microscopy. Nature 259: 508-510

Joseleau JP, Ruel K, 1997. Study of lignification by noninvasive techniques in growing maize inter- nodes An investigation by Fourier transform in-

frared cross-polarization-magic angle spinning 13C-nuclear magnetic resonance spectroscopy and immunocytochemical transmission electron microscopy. Plant Physiol 114: 1123-1133

Jung HG, Casler MD, 2006. Maize stem tissues: Impact of development on cell wall degradability. Crop Sci 46: 1801-1809

Kerk NM, Ceserani T, Tausta SL, Sussex IM, Nelson V, 2003. Laser capture microdissection of cells from plant tissues. Plant Physiol 132: 27-35

Kieran JD, Susan E, Knox JP, 2011. Cell wall biology: perspectives from cell wall imaging. Molecular Plant 4: 212-219

Knox JP, 2008. Revealing the structural and functional diversity of plant cell walls. Curr Opin Plant Biol 11: 308-313

McCann MC, Defernez M, Urbanowicz BR, Tewari JC, Langewisch T, Olek A, Wells B, Wilson RH, Carpita NC, 2007. Neural network analyses of infrared spectra for classifying cell wall architectures. Plant Physiol 143: 1314-1326

McCann MC, Hammouri M, Wilson R, Belton P, Roberts K, 1992. Fourier transform infrared microspectroscopy is a new way to look at plant cell walls. Plant Physiol 100: 1940-1947

McManus WR and Bigham ML, 1973. Studies on forage cell walls. J Agric Sci 80: 283-296

Méchin V, Argillier O, Rocher F, Hebert Y, Mila I, Pollet B, Barriere Y, Lapierre C, 2005. In search of a maize ideotype for cell wall enzymatic degradability using histological and biochemical lignin characterization. J Agric Food Chem 53: 5872-5881

Morrison TA, Jung HG, Buxton DR, 1996. Degradability of cell-wall constituents in corn internodes during stalk development, pp 83-84. US Dairy Forage Research Center

Morrison TA, Jung HG, Buxton DR, Hatfield RD, 1998. Cell-wall composition of maize internodes of varying maturity. Crop Sci 38: 455-460

Morrison TA, Kessler JR, Hatfield RD, Buxton DR, 1994. Activity of two lignin biosynthesis enzymes during development of a maize internode. J Sci Food Agric 65: 133-139

Müsel G, Schindler T, Bergfeld R, Ruel K, Jacquet G, Lapierre C, Speth V, Schopfer P, 1997. Structure and distribution of lignin in primary and secondary cell walls of maize coleoptiles analyzed by chemical and immunological probes. Planta 201: 146-159

Nakashima J, Chen F, Jackson L, Shadle G, Dixon RA, 2008. Multi-site genetic modification of monolignol biosynthesis in alfalfa (*Medicago sativa*): effects on lignin composition in specific cell types. New Phytol 179: 738-750

Nakazono M, Qiu F, Borsuk LA, Schnable PS, 2003. Laser-capture microdissection, a tool for the global analysis of gene expression in specific plant cell types: identification of genes expressed differentially in epidermal cells or vascular tissues of maize. Plant Cell 15: 583-596

Philippe S, Robert P, Barron C, Saulnier L, Guillon F, 2006. Deposition of cell wall polysaccharides in wheat endosperm during grain development: Fourier transform-infrared microspectroscopy study. J Agric Food Chem 54: 2303-2308

Philippe S, Tranquet O, Utille JP, Saulnier L, Guillon F, 2006. Investigation of ferulate deposition in endosperm cell walls of mature and developing wheat grains by using a polyclonal antibody. Planta 225: 1287-1299

Ruel K, Berrio-Sierra J, Derikvand MM, Pollet B, Thevenin J, Lapierre C, Jouanin L, Joseleau JP, 2009. Impact of CCR1 silencing on the assembly of lignified secondary walls in *Arabidopsis thaliana*. New Phytol 184: 99-113

Schertz KF, Rosenow DT, 1977. Anatomical variation in stalk internodes of sorghum crop. Science 17: 628-631

Séné C, McCann MC, Wilson RH, Grinter R, 1994. Fourier-Transform Raman and Fourier-Transform Infrared Spectroscopy (An investigation of five higher plant cell walls and their components). Plant Physiol 106: 1623-1631

Tamasloukht B, Wong Quai Lam MS, Martinez Y, Tozo K, Barbier O, Jourda C, Jauneau A, Borderies G, Balzergue S, Renou JP, Huguet S, Martinant JP, Tatout C, Lapierre C, Barriere Y, Goffner D, Pichon M, 2011. Characterization of a *cinnamoyl-CoA reductase 1* (*CCR1*) mutant in maize: effects on lignification, fibre development, and global gene expression. J Exp Bot 62: 3837-3848

Walters RJK, 1971. Variation in the relationship between in vitro digestibility and voluntary dry-matter intake of different grass varieties. J Agric Sci 76: 243-252

Wilkins RJ, 1972. The potential digestibility of cellulose in grasses and its relationship with chemical and anatomical parameters J Agric Sci 78: 457-464